

Inclusions in large diamond single crystals at different temperatures of synthesis

Fei Han(韩飞), Shang-Sheng Li(李尚升), Xue-Fei Jia(贾雪菲), Wei-Qin Chen(陈玮琴), Tai-Chao Su(宿太超), Mei-Hua Hu(胡美华), Kun-Peng Yu(于昆鹏), Jian-Kang Wang(王健康), Yu-Min Wu(吴玉敏), Hong-An Ma(马红安), Xiao-Peng Jia(贾晓鹏)

Citation: Chin. Phys. B . 2019, 28(2): 028103. **doi:** 10.1088/1674-1056/28/2/028103
Journal homepage: http://cpb.iphy.ac.cn; http://iopscience.iop.org/cpb

What follows is a list of articles you may be interested in

Synthesis of diamonds in Fe—C systems using nitrogen and hydrogen co-doped impurities under HPHT

Shi-Shuai Sun(孙士帅), Zhi-Hui Xu(徐智慧), Wen Cui(崔雯), Xiao-Peng Jia(贾晓鹏), Hong-An Ma(马红安)
Chin. Phys. B . 2017, 26(9): 098101. **doi:** 10.1088/1674-1056/26/9/098101

Different effect of NiMnCo or FeNiCo on the growth of type-IIa large diamonds with Ti/Cu as nitrogen getter

Shang-Sheng Li(李尚升), He Zhang(张贺), Tai-Chao Su(宿太超), Qiang Hu(胡强), Mei-Hua Hu(胡美华), Chun-Sheng Gong(龚春生), Hon-An Ma(马红安), Xiao-Peng Jia(贾晓鹏), Yong Li(李勇)
Chin. Phys. B . 2017, 26(6): 068102. **doi:** 10.1088/1674-1056/26/6/068102

Synthesis of N-type semiconductor diamonds with sulfur, boron co-doping in FeNiMnCo-C system at high pressure and high temperature

He Zhang(张贺), Shangsheng Li(李尚升), Taichao Su(宿太超), Meihua Hu(胡美华), Hongan Ma(马红安), Xiaopeng Jia(贾晓鹏), Yong Li(李勇)
Chin. Phys. B . 2017, 26(5): 058102. **doi:** 10.1088/1674-1056/26/5/058102

High thermal stability of diamond-cBN-B_4C-Si composites

Hong-Sheng Jia(贾洪声), Pin-Wen Zhu(朱品文), Hao Ye(叶灏), Bin Zuo(左斌), Yuan-Long E(鄂元龙), Shi-Chong Xu(徐仕翀), Ji Li(李季), Hai-Bo Li(李海波), Xiao-Peng Jia(贾晓鹏), Hong-An Ma(马红安)
Chin. Phys. B . 2017, 26(1): 018102. **doi:** 10.1088/1674-1056/26/1/018102

Large single crystal diamond grown in FeNiMnCo-S-C system under high pressure and high temperature conditions

He Zhang(张贺), Shangsheng Li(李尚升), Taichao Su(宿太超), Meihua Hu(胡美华), Guanghui Li(李光辉), Hongan Ma(马红安), Xiaopeng Jia(贾晓鹏)
Chin. Phys. B . 2016, 25(11): 118104. **doi:** 10.1088/1674-1056/25/11/118104

Inclusions in large diamond single crystals at different temperatures of synthesis*

Fei Han(韩飞)[1], Shang-Sheng Li(李尚升)[1,†], Xue-Fei Jia(贾雪菲)[1], Wei-Qin Chen(陈玮琴)[1], Tai-Chao Su(宿太超)[1], Mei-Hua Hu(胡美华)[1], Kun-Peng Yu(于昆鹏)[1], Jian-Kang Wang(王健康)[1], Yu-Min Wu(吴玉敏)[1], Hong-An Ma(马红安)[2], and Xiao-Peng Jia(贾晓鹏)[2]

[1] *School of Materials Science and Engineering, Henan Polytechnic University, Cultivating Base for Key Laboratory of Environment-friendly Inorganic Materials in University of Henan Province, Jiaozuo* 454000, *China*

[2] *State Key Laboratory of Superhard Materials, Jilin University, Changchun* 130012, *China*

(Received 6 September 2018; revised manuscript received 28 November 2018; published online 10 January 2019)

The inclusions in large diamond single crystals have effects on its ultimate performance, which restricts its industrial applications to a great extent. Therefore, it is necessary to study the inclusions systematically. In this paper, large diamond single crystals with different content values of inclusions are synthesized along the (100) surface by the temperature gradient method (TGM) under 5.6 GPa at different temperatures. With the synthetic temperature changing from 1200 °C to 1270 °C, the shapes of diamonds change from plate to low tower, to high tower, even to steeple. From the microscopic photographs of the diamond samples, it can be observed that with the shapes of the samples changing at different temperatures, the content values of inclusions in diamonds become zero, a little, much and most, correspondingly. Consequently, with the temperature growing from low to high, the content values of inclusions in crystals increase. The origin of inclusions is explained by the difference in growth rate between diamond crystal and its surface. The content values of inclusions in diamond samples are quantitatively calculated by testing the densities of diamond samples. And the composition and inclusion content are analyzed by energy dispersive spectroscopy (EDS) and x-ray diffraction (XRD). From contrasting scanning electron microscopy (SEM) photographs, it can be found that the more the inclusions in diamond, the more imperfect the diamond surface is.

Keywords: inclusions, large diamond single crystals, high pressure and high temperature

PACS: 81.05.ug, 61.72.S–, 61.05.C–, 61.72.Ff **DOI:** 10.1088/1674-1056/28/2/028103

1. Introduction

As a functional material with many ultimate uses, diamond has applications in many fields.[1–8] At present, the main synthetic method of diamond growth is the high pressure and high temperature (HPHT) static pressure method using metal catalyst as medium.[9–11] Generally, graphite dissolves in the melt of alloy catalysts, whose components are Fe, Ni, Co, Mn, Cr, *etc*., and precipitates to grow as diamond under HPHT. It is difficult to avoid trapping some metallic impurities in crystals.[12] These impurities are usually called inclusions which exist in gaseous and solid forms.[11] The inclusions affect many properties of diamond crystal,[13] especially thermal stability.[14] At the same time, inclusions are also an important way to study the conditions of diamond growth, such as temperature and pressure.[15] Therefore, the study of inclusions has always been a focus of attention in the field of diamond research.[16–18]

The inclusions in synthetic diamond can usually be classified as gaseous inclusions and solid inclusions according to their existence forms. Further, the solid inclusions are divided into graphite inclusions and metal inclusions.[19] It is found from the growth process of diamonds that there are two ways the inclusions exist in the crystal: one is the initial inclusions formed at the beginning of the diamond growth, and the other is the interaction among the impurities themselves in the process of the diamond formation and growth.[20] In addition, the compositions of alloy catalysts have a great influence on the formation of inclusions. It is found from the study of Moss Fort spectrum that the inclusions are usually metal impurities or metastable carbides.[21–24]

Currently, the research on inclusions in abrasive grade diamonds is more mature than in large diamond single crystals. In this paper, the large diamond single crystals are synthesized along the (100) surface at different temperatures under high pressure, in which the inclusions can be studied.

2. Experiments

Large diamond single crystals were synthesized by TGM (Fig. 1) under HPHT in a China-type cubic high pressure apparatus (CHPA) (SPD-6 × 1200). The temperature gradients

*Project supported by the Natural Science Foundation of Henan Province, China (Grant No. 182300410279), the Key Science and Technology Research Project of Henan Province, China (Grant No. 182102210311), the Key Scientific Research Project in Colleges and Universities of Henan Province, China (Grant No. 18A430017), the Professional Practice Demonstration Base Program for Professional Degree Graduate in Material Engineering of Henan Polytechnic University, China (Grant No. 2016YJD03), and the Fund for the Innovative Research Team (in Science and Technology) in the University of Henan Province, China (Grant No. 19IRTSTHN027).

†Corresponding author. E-mail: lishsh@hpu.edu.cn

© 2019 Chinese Physical Society and IOP Publishing Ltd

were kept the same for achieving repeatability of assembly for all the samples, thereby ensuring that except temperature all the conditions relating to growth rate were the same. Under the same assembly, the different shapes of diamonds were grown at different synthetic temperatures.

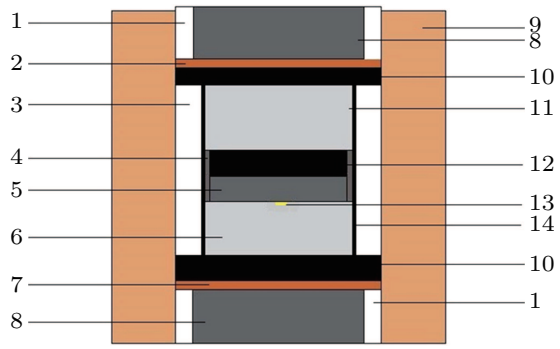


Fig. 1. Schematic diagram of TGM. 1: pyrophyllite ring, 2: copper sheet, 3: salt tube, 4: insulating ring, 5: catalyst, 6: crystal bed, 7: copper sheet, 8: steel cap, 9: pyrophyllite, 10: carbon sheet, 11: plug, 12: carbon source, 13: seed crystal, and 14: graphite tube.

High-purity artificial graphite was selected as the carbon source and FeNi alloy ($Fe_{64}Ni_{36}$, subscript number was percentage of mass, abbreviated FeNi) was selected as catalyst. High-quality cuboctahedral diamond crystals each with a diameter of about 0.6 mm, which were synthesized by film growth method under HPHT, were selected to use as seeds. One (100) crystal plane was used as the initial crystal growth surface. Large diamond single crystals with different shapes were synthesized, in which the growth time was controlled to be 10 h, under a pressure of about 5.6 GPa and the temperature ranging from 1200 °C to 1270 °C. The collected samples were treated in a boiling mixture of H_2SO_4 and HNO_3 to remove remnant graphite and catalyst. Then, the collected samples were cleaned in boiling deionized water.

In these experiments, the temperature was measured by a Pt-30% Rh/Pt-6% Rh thermocouple. In order to ensure the accuracy and repeatability of temperature measurement, the preparation of each part for assemble was made by a rigorous process and the location of temperature measurement was ensured by special tools. The pressure was estimated by load of oil press, which was calibrated by a curve that was established on the pressure-induced phase transitions of elements of Bi, Ba, and Tl.[4]

The color, morphology, and inclusions of large diamonds were characterized by taking photos under optical microscope. The sizes of samples were measured with a Vernier caliper. A high precision electronic balance (accurate to 0.01 mg) was used to weigh the mass of diamond samples. SEM was used to observe the surfaces of samples. The specific gravity balance (FA2104J) was used to measure the mass of the samples in the air and water, and then the density of each sample was calculated by Archimedes method. The composition of inclusions was tested by EDS. Subsequently, the inclusions in the diamond samples were analyzed according to these characteristics.

3. Results and discussion

3.1. Effect of temperature on inclusions in diamond

Diamonds are synthesized at different temperatures by selecting the (100) surface of the seed as the growth surface. The growth time is 10 h. Four diamond samples are selected from many synthetic diamond samples to be discussed as representative, which are numbered A, B, C, and D. The synthesis conditions and results of these four samples are shown in Table 1. The corresponding diamond crystal images are shown in Fig. 2. In this study, the β value is used to describe the crystal shape in detail. Here, the β value is the ratio of height to diameter of diamond crystal. Figure 3 shows the schematic diagram of the β value.[6]

Table 1. Experimental results of large diamonds at different temperatures.

Number	Temperature/°C	Crystal weight/mg	Growth rate/mg·h^{-1}	Crystal shape	β values
A	1200	23.95	2.395	plate	0.48
B	1220	26.85	2.685	low tower	0.52
C	1260	33.77	3.377	high tower	0.74
D	1270	36.28	3.628	steeple	0.97

The results of four diamonds seen in Table 1 are synthesized at temperatures of 1200, 1220, 1260, and 1270 °C, respectively. There are two optical micrographs of each sample with different orientations (vertical view and front view) in Fig. 2. It can be seen from Figs. 2(a) and 2(a*) that sample A is in the shape of plate, it is yellow and transparent and contains no inclusion. Sample B is in the shape of low tower, it is yellow and transparent and contains a small number of inclusions scattered inside (seen in Figs. 2(b) and 2(b*)). Figures 2(c) and 2(c*) show that sample C is in the shape of high tower, it is yellow and transparent and contains black solid inclusions that concentrate in the central core and extend in the columnar form longitudinally. Sample D is steeple-shaped, it is yellow and poorly transparent and contains a large number of black

solid inclusions. It can be observed from Fig. 2(d) that there is a series of inclusions in the center of sample D, and the inclusions are unevenly distributed outside the center. Figure 2(d*) shows that its inclusions are flaky or cluster-like. Comparison between Figs. 2(d*) and 2(c*) shows that the inclusions in sample C are significantly less than those in sample D.

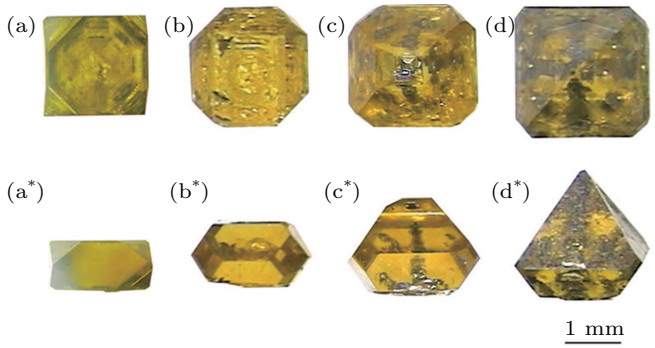


Fig. 2. (a)–(d) Vertical-view and (a*)–(d*) front-view micrographs of diamond samples under optical microscope.

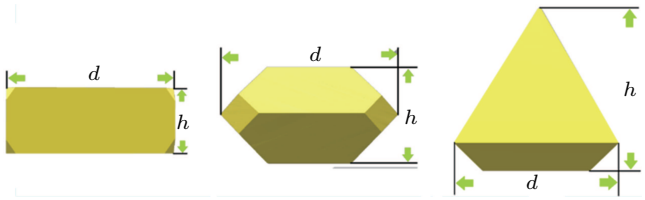


Fig. 3. Schematic diagram of β value.

The experimental results show that for large single diamond crystals growing along the (100) surface, the normal growth rate along the (100) surface increases gradually with the temperature increasing from low to high, and the inclusion content increases in turn as the crystal shape changes from plate, low tower, high tower to steeple.

The difference among inclusion content values in diamonds grown at different temperatures can be explained by their growth rates. The diamond samples (Fig. 2) are synthesized by using TGM under the same assembly condition, which confirms that the temperature gradients are the same for all the samples in the growing process. The only difference is the temperature, which should be responsible for different morphological characteristics of the samples. When the (100) surface is used as the starting surface for the diamond growth, the growth for high-quality crystal favors low temperature. When the temperature increases, the crystal will exhibit a large (111) surface, which suggests that the growth rate along the normal direction of (100) surface should become larger. That is, the increase in temperature can enhance the growth rate along the direction perpendicular to the (100) surface although the temperature gradients around the crystal are the same. Therefore, the larger growth rate will lead to more inclusions during the (100) surface shrinking and disappearing.

The shape changes of the diamonds prepared at different synthetic temperatures conform to the principle of "slow surface expose and fast surface submergence.[25]" At the same time, the changes of growth rate in the different surfaces of diamonds at different synthetic temperatures also conform to the law of "the axial growth rate of diamond (100) face from slow to fast with the temperature increasing from low to high.[26,27]" Combining the above analysis of inclusions in samples A, B, C, and D, it can be obtained that the faster the axial growth rate of (100) surface, that is, the faster the normal stacking rate, the greater the number of inclusions in the crystal and the worse the transparency of the diamond.

In addition, it can be seen from the overall growth rate of diamond samples in Table 1 that the growth rate of samples A, B, C, and D increase in turn. Based on the law of "the faster the growth rate of diamond, the more unfavorable the high-quality single crystal obtained is.[25]" It seems that the overall growth rate is another reason for the inclusion increase. However, we think that the reasons for the increase in the overall growth rate of diamond samples are both the change of shape and the appearance of the inclusions. The reason for the change of shape from plate to tower then to steeple is in common with the reason for the change of normal growth rate of (100) surface. The other reason for the appearance of the inclusions is because the density of inclusion is more than that of diamond. Therefore, the increase for the overall growth rate of the diamond sample is the indirect cause for the increase of inclusions.

3.2. Composition and structure of inclusions in diamond

The inclusions in the cracked sample D are tested by EDS and XRD, respectively.

The inclusions are in the diamond crystal and usually exist in quite a small quantity, so it is difficult to analyze by common surface analysis methods. In order to test the compositions of inclusions in diamond, the samples are broken into fragments (Figs. 4(a) and 4(b)) for EDS. The curve of inclusion compositions is shown in Fig. 4(c). The test results are listed in Table 2. As shown in Table 2, the main components of inclusions are Fe, Ni, and a small quantity of C elements. Inclusions are formed by the catalyst melt and the C elements involved in the growth of diamond crystals.

Figure 5 shows the XRD test of the inclusions in diamond. It shows that the inclusions are f.c.c. $(FeNi)_{23}C_6$ and Ni_3C.

The above results of the inclusion compositions and structure are similar to those presented by Yin *et al.*[11,16] in which the inclusions in diamond are found to be composed of f.c.c. $(FeNi)_{23}C_6$.

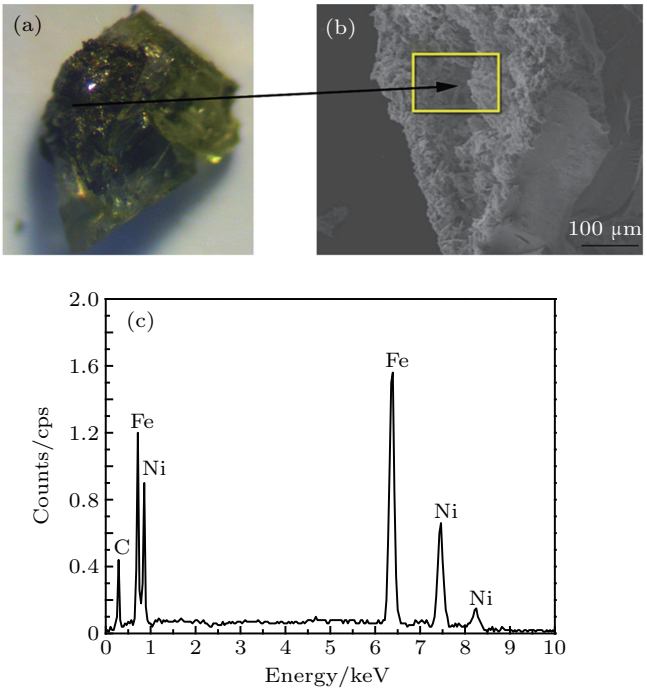


Fig. 4. EDS test of the inclusions in (a) shattered crystal, (b) enlarged view of inclusions, and (c) curve of inclusion compositions.

Table 2. Compositions of inclusions in diamond by EDS test.

Element	C	Fe	Ni	Total
wt%	8.50	53.10	38.40	100.00

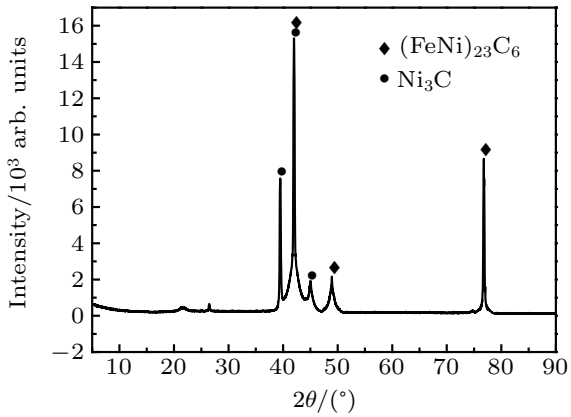


Fig. 5. XRD test of the inclusions in diamond.

Although the composition of the inclusions is revealed, the growth mechanisms of diamond and the catalytic effect of the metal are still a matter of discussion.[14] For the compositions of the inclusions given in Table 2, the ratio between Fe and Ni is different from that in the starting catalyst. This might be due to the uneven concentration of metal carbides in the FeNi catalyst. In the process of diamond crystal growth, the liquid iron–nickel that dissolves carbon or iron–nickel carbide is introduced into the diamond, the iron–nickel reacts with graphite trapped in the diamond and the diamond forms carbide below its melting point. As residual liquid FeNi is cooled further, it would eject carbon continuously to the walls of the cavity until it becomes the Fe–Ni–C eutectic composition. The iron–nickel carbide reacts continuously with graphite or diamond. As the temperature decreases further, the metallic inclusions solidify, and the compound of inclusions is left.[16]

3.3. Content of inclusions in diamond

In order to accurately determine the inclusion content in diamond crystal, it is calculated by measuring the density of inclusions and diamond.

In order to reduce the error of density test, the experiments are carried out five times for each sample. The maximum and minimum values are removed from the five sets of density data for each crystal sample, and the average values are calculated from the remaining three sets of data, and are shown in Table 3.

Table 3. Average sample density and inclusion percentage of total volume.

Sample	A	B	C	D
Averages ρ/(g/cm^3)	3.5043	3.5133	3.5571	3.6054
$V_I/(V_I+V_D)$	0	0.23%	1.33%	2.55%

Because inclusions are mostly composed of Fe and Ni, their densities are much higher than diamond density. The increase of inclusion content will lead to the increase of sample density. It is found from Table 3 that the densities of samples A, B, C, and D increase in turn, which accords with the law of inclusion content described in the previous section.

It can be obtained from Table 3 that the densities of four samples can be measured to be $\rho_D = \rho_{(a)} = 3.5043$ g/cm^3 (sample A without inclusions), $\rho_{(b)} = 3.5133$ g/cm^3, $\rho_{(c)} = 3.5571$ g/cm^3, and $\rho_{(d)} = 3.6054$ g/cm^3.

In order to quantitatively analyze the content of inclusions, the density of inclusions should be measured. Inclusions are collected after diamond sample D with the highest inclusion content has been smashed. Then its density was tested five times and finally obtained to be $\rho_I = 7.4666$ g/cm^3.

Assuming that the volume of inclusions in diamond is V_I (density $\rho_I = 7.4666$ g/cm^3), the volume of remaining diamond is V_D (density $\rho_D = \rho_{(a)} = 3.5043$ g/cm^3), and the density of diamond containing inclusions is ρ, the percentage of inclusions relative to total volume of diamond with inclusions can be calculated. Because the mass of inclusions contained in the diamond is equal to the sum of the inclusion mass and the diamond mass, the equation is obtained as follows:

$$\rho\,(V_I+V_D) = (\rho_D V_D + \rho_I V_I)\,. \tag{1}$$

The variation formula is

$$V_I/V_D = (\rho-\rho_D)\,/\,(\rho_I-\rho)\,. \tag{2}$$

The percentage of inclusion volume relative to total volume of diamond with inclusions is as follows:

$$V_{\mathrm{I}}/(V_{\mathrm{I}}+V_{\mathrm{D}}) = (V_{\mathrm{I}}/V_{\mathrm{D}})/(1+V_{\mathrm{I}}/V_{\mathrm{D}}). \tag{3}$$

Equation (2) is substituted into Eq. (3) and the resulting expression is given as follows:

$$V_{\mathrm{I}}/(V_{\mathrm{I}}+V_{\mathrm{D}}) = (\rho-\rho_{\mathrm{D}})/(\rho_{\mathrm{I}}-\rho_{\mathrm{D}}). \tag{4}$$

The density of each diamond sample is measured and given in the second row of Table 3. The percentages of inclusions in the volumes of samples A, B, C, and D are calculated in turn and the results are shown in line 3 of Table 3.

The results of the inclusion content in Table 3 accurately indicate the percentage of inclusions in the total volume of each diamond sample. As can be seen from Table 3, the percentages of inclusions in the volume of the four samples A, B, C, and D are, 0%, 0.23%, 1.33%, and 2.55%, respectively. Namely, with the increase of the synthesis temperature, the content of inclusions increases, which is in accord with the result of the discussion in Subsection 3.1.

3.4. Surface conditions of diamond crystals with different content of inclusions

When diamond crystals grow too fast, carbon atoms pile up so fast that the impurities cannot be discharged. Subsequently, impurities are trapped to form inclusions. The existence of inclusions will inevitably affect the surface of diamond crystal, which is closely related to the quality of the diamond crystal. In order to study the effect of inclusion content on the surface of diamond crystal, the SEM images (as shown in Fig. 6, with all SEM images magnified 1000 times.) are taken at the (100) or (111) surface for the four diamond crystals (Fig. 2).

Firstly, the following results are found by comparing the patterns of images (a_1), (b_1), (c_1) and (d_1), which are taken at the (100) plane. The crystal surface of image (a_1) presents a growth pattern like leaves. And the dendritic growth pattern appears on the crystal surface in image (b_1). Next, the crystal surfaces in images (c_1) and (d_1) are full of etched pits most of which shapes are quadrangles and the rest are irregular. The number of etched pits in image (d_1) is higher than that in image (c_1). It is concluded that with the increase of the inclusion content, the (100) surface gradually changes from regular smooth leaves to rough dense pits.

Secondly, the surface patterns of (111) plane, which appear in images (a_2), (b_2), (c_2) and (d_2) in Fig. 6, are compared and analysed. The diamond crystal facet in image (a_2) is smooth and has sporadic "circular shallow pits". Then, the (111) surface of sample B in image (b_2) shows visible "flushing stripes". Further, the (111) surface of samples C and D (image (c_2) and (d_2)) is full of "pyramidal pits,[28]" and the number of etched pits in image (d_2) were more than that in image (c_2). The pyramidal pits are different from the "trigons", which come from varieties of positive and negative orientations with respect to an octahedral face: point-bottomed and flat-bottomed, steep-sided and shallow-sided.[29,30] Furthermore, the zigzag growth layer can also be observed in image (c_2). It can be concluded that with the increase of inclusion content in the diamond sample, the (111) surface develops from "circular shallow pits" to "flushing stripes", then etched pits appear, until more etched pits cover the whole facet.

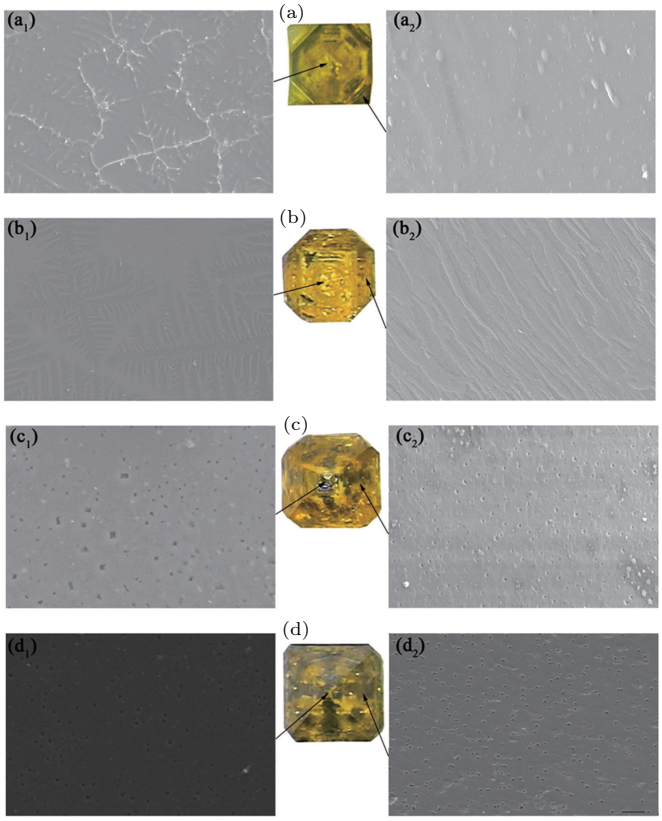


Fig. 6. SEM images of diamond surfaces taken at [(a_1)–(d_1)] (100) plane and [(a_2)–(d_2)] (111) plane for corresponding diamonds.

As described, for diamond samples A and B in which the inclusion content is below 0.23% in Table 3, whether the "leafy" and "dendritic" stripes are on the (100) plane or the "circular shallow pits" and "flushing stripes" are on the (111) planes, these patterns should be caused by the deposition of carbon atoms between the metal catalyst textures in the condensation process of diamond.[25] When the β values of samples A and B (Table 1) are both less than 0.52, the growth rate on (111) plane is faster than that on (100) plane and the different atomic structures on the (100) and (111) surface result in the different surface shapes of (100) and (111) in samples A and B.

In addition, for diamond samples C and D in which inclusion content is higher than 1.33% in Table 3, the "quadrilateral" and "irregular" pits on the (100) plane and the "pyramidal pits" pits on the (111) plane are found. These pits occur

at the position where impurities are difficult to remove during the growth of diamond crystals. And these pits emerge by the dissolution of metallic impurities in the acid treatment. When the β value of samples C and D (Table 1) are both higher than 0.74, the growth rate on (100) surface is faster than that on (111) plane and the different atomic structures on the (100) and (111) surface result in the different surface shapes of planes (100) and (111) in samples C and D. No matter (100) or (111) plane, the etch pits of sample D are also more than in sample C. That is because the inclusion content of sample D is more than that of sample C.

4. Conclusions

By studying the inclusions of large diamond crystals along the (100) plane at different temperatures, the conclusions are obtained as follows:

(i) The inclusion content increases gradually as the temperature changes from low to high, and the crystal shape changes from plate, low tower, high tower to steeple. The plate shape of large diamond crystal, which is synthesized at low temperature, is high-quality diamond with no inclusions.

(ii) It is shown by EDS that the inclusions trapped in diamond are composed of Fe, Ni and a small quantity of C elements.

(iii) The inclusion content in diamond is quantitatively calculated by measuring the density of inclusions and diamond.

(iv) The greater the number of inclusions in the diamond, the greater the number of pits on the crystal surface, the fewer inclusion, and the smoother the crystal surface.

References

[1] Li S S, Ma H A, Li X L, Su T C, Huang G F, Li Y and Jia X P 2011 *Chin. Phys. B* **20** 028103

[2] Sumiya H, Toda N and Satoh S 2002 *J. Crystal Growth* **237–239** 1281

[3] Sumiya H, Toda N, Nishibayashi Y and Satoh S 1997 *J. Crystal Growth* **178** 485

[4] Li Y, Jia X P, Shi W, Leng S L, Ma H A, Sun S S, Wang F B, Chen N and Long Y 2014 *Int. J. Refract. Met. Hard Mater.* **43** 147

[5] Li Z C, Jia X P, Huang G F, Hu M H, Li Y, Yan B M and Ma H A 2013 *Chin. Phys. B* **22** 014701

[6] Xiao H Y, Jia X P, Zang C Y, Li S S, Tian Y, Zhang Y F, huang G F, Ma L Q and Ma H A 2008 *Chin. Phys. Lett.* **25** 1469

[7] Hu M H, Li S S, Ma H A, Su T C, Li X L, Hu Q and Jia X P 2012 *Chin. Phys. B* **21** 098101

[8] Zhang H, Li S S, Su T C, Hu M H, Li G H, Ma H A and Jia X P 2016 *Chin. Phys. B* **25** 118104

[9] Novikov N V 1999 *Diam. Relat. Mater.* **8** 1427

[10] Zhang H, Li S S, Su T C, Hu M H, Ma H A, Jia X P and Li Y 2017 *Chin. Phys. B* **26** 058102

[11] Yin L W, Li M S, Sun D S and Cui J J 2001 *Mater. Lett.* **48** 21

[12] Zhou L, Jia X P, Ma H A, Zheng Y J and Li Y T 2008 *Chin. Phys. B* **17** 4665

[13] Gong C S, Li S S, Zhang H R, Su T C, Hu M H, Ma H A, Jia X P and Li Y 2017 *Int. J. Refract. Met. Hard Mater.* **66** 116

[14] Langenhorst F, Poirier J P and Forst D J 2004 *J. Mater. Sci.* **39** 1865

[15] Yin L W, Wang N W, Zou Z D, Li M S, Sun D S, Zheng P Z and Yao Z Y 2000 *Appl. Phys. A* **71** 473

[16] Yin L W, Zou Z D, Li M S, Liu Y X, Cui J J and Hao Z Y 2000 *Mater. Sci. Eng. A* **293** 107

[17] Chen L X and Li X Y 2004 *J. Gems Gemmol.* **6** 25 (in Chinese)

[18] Neuser R D, Schertl H P, Logvinova A M and Sobolev N V 2015 *Russ. Geol. Geophys.* **56** 321

[19] Khokhryakov A F and Nechaev D V 2015 *Russ. Geol. Geophys.* **56** 232

[20] Angel R J, Alvaro M, Nestola F and Mazzucchelli M L 2015 *Russ. Geol. Geophys.* **56** 211

[21] Bharuth-Ram K and Hansen M F 2002 *Physica B* **321** 29

[22] Eaton-Magaña S, Ardon T and Zaitsev A M 2017 *Diamond Relat. Mater.* **71** 20

[23] Nestola F, Cerantola V, Milani S, Anzolini C, McCammon C, Novella D, Kupenko I, Chumakov A, Rüffer R and Harris J W 2016 *Lithos* **265** 328

[24] Ma H A, Jia X P, Chen L X, Zhu P W, Guo W L, Guo X B, Wang Y D, Li S Q, Zou G T, Zhang G and Bex P 2002 *J. Phys.: Condens. Matter* **14** 11269

[25] Zhang H, Li S S, Su T C, Hu M H, Zhou Y M, Fan H T, Gong C S, Jia X P, Ma H A and Xiao H Y 2015 *Acta Phys. Sin.* **64** 198103 (in Chinese)

[26] Zhang Y, Dong F X, Wan S Q, Xie X J, Gong L J, Wang Y F and Qiu L X 2011 *J. Jilin Univ. Sci. Ed.* **49** 935 (in Chinese)

[27] Wang J Z, Li S S, Su T C, Hu M H, Hu Q, Wu Y M, Wang J K, Han F, Yu K P, Gao G J, Guo M M, Jia X P, Ma H A and Xiao H Y 2018 *Acta Phys. Sin.* **67** 168101 (in Chinese)

[28] Sun S S, Jia X P, Yan B M, Wang F B, Li Y D, Chen N and Ma H A 2014 *Diamond Relat. Mater.* **42** 21

[29] Agrosì G, Nestola F, Tempesta G, Bruno M, Scandale E and Harris J 2016 *Lithos* **248–251** 153

[30] Moore M, Nailer S G and Wierzchowski W K 2016 *Crystals* **6** 71